# MODIFICATION OF MAGNETIC SIGNALS OF SHORT-PERIOD PULSATIONS BY THE IONOSPHERE

Shigeru FUJITA

*Kakioka Magnetic Observatory, 595, Kakioka, Yasato-machi, Niihari-gun, Ibaraki 315-01*

*Abstract:* The transmission, mode conversion, and reflection of HM-waves associated with short-period geomagnetic pulsations through and by the ionosphere are comparatively examined for three different model cases, bearing in mind the localized injection of the shear Alfvén wave at high latitude and the consequent horizontal spread of disturbances to low-latitude regions through the ducted propagation in the upper ionosphere. In the first model case composed of two semi-infinite layers (the magnetosphere and the neutral atmosphere) with a separating interface (the ionospheric *E*-layer with anisotropic conductivities), we have studied conductivity dependences of the transmission of magnetic signals of the shear Alfvén and the fast magnetosonic waves respectively, propagating down along vertical field lines and having a periodic horizontal structure. For the Alfvén wave incidence with the static electric field the transmitted magnetic signal intensity has a peak against the Hall conductivity variation, while it rather decreases as the Pedersen conductivity increases. We have also shown that the ionosphere behaves as a shielding metalic conductor for the incidence of the fast magnetosonic wave with the inductive electric field. In the second model case consisting of five layers, *i.e.* a magnetospheric region, an upper ionosphere as a trapping region, an interface (*E*-region), an atmospheric region, and a semi-infinite solid earth, we have dealt with ionospheric effects on a localized incidence of the shear Alfvén wave. A comparison of magnetic signal intensities at the levels just above and below the *E*-layer leads us to conclude that the behaviour of magnetic signals in a near-source region is similar to that obtained in the first model case without a trapping region, and that the dominating direct source of ground magnetic fields is the induced eddy Hall current in the ionosphere. Finally, the ionospheric shielding effect in a distant region from the injection source has been estimated by employing the third model of the ducted propagation of the fast magnetosonic wave in the upper ionosphere. We conclude that the ionospheric screening is rather significant in the source region when the Pedersen to Hall conductivity ratio is much larger than unity while it is not so significant in the intermediate and distant regions.

## 1. Introduction

One of the basic problems for study of geomagnetic pulsations is that how hydromagnetic (HM) waves are modified through interaction with an anisotropic conducting ionosphere. Many workers have devoted themselves to theoretical study on the HM-wave reflection by and transmission through the ionosphere (*cf.*, NISHIDA, 1964; TAMAO, 1964; C. GREIFINGER and P. GREIFINGER, 1965). Using a simplified ionosphere model with height-integrated anisotropic conductivities and assuming an oblique propagation plane of HM-wave to the vertical field line, NISHIDA (1964) estimated the ionospheric screening effect of magnetic signals in a case of the Alfvén wave incidence. He also showed that the rotation of the principal axis of the horizontal magnetic field vector by $\pi/2$ is taking place during a passage through the ionosphere. TAMAO (1964) examined the ionospheric response to the vertical incidence of the shear Alfvén wave with a periodic horizontal structure, and concluded that the direct source of the associated magnetic field on the ground is the induced eddy Hall current whereas the toroidal magnetic field due to the Pedersen current is negligible. After the pioneering works mentioned above, the succeeding study has dealt with this basic problem with a more realistic ionospheric model (*e.g.*, C. GREIFINGER and P. GREIFINGER, 1965).

On the other hand, dispersion characteristics including the absorption rate of the ducted horizontal propagation of the short-period fast magnetosonic wave in the ionosphere were investigated by many workers in relation to the origin of pc-1 pulsations observed at low latitudes (*e.g.*, C. GREIFINGER and P. GREIFINGER, 1968; P. GREIFINGER, 1972). Recently, FUJITA and TAMAO (1984, 1985) and FUJITA (1985) have studied in detail the ionospheric response to the localized incidence of the shear Alfvén wave at high latitudes, by making use of a horizontally stratified model with a trapping duct layer. In the present paper, to obtain different response characteristics of the ionosphere our attention will be focussed mainly on the transmission of short-period magnetic signals, which are taking place in three typical regions, *i.e.*, a near-source region, a region far away from the injection source, and an intermediate one between the two.

## 2. Modification of Incident HM-Waves by the Ionosphere

### 2.1. *A simple injection model without a trapping layer*

Before attempting to examine ionospheric effects on a localized incident shear Alfvén wave in high latitudes and the horizontal spread of the secondarily generated magnetosonic waves by the induced Hall current in a model ionosphere with a trapping duct region, let us consider different response behaviour of the ionosphere for two cases of the vertical incidence of HM-waves with a horizontal periodic structure, *i.e.*, the shear Alfvén and the fast magnetosonic waves (hereafter we call it the fast wave), by adopting the simplest model consisting of two semi-infinite layers separated by an interface (ionospheric *E*-layer with height-integrated Pedersen and Hall conductivities, $\Sigma_P$ and $\Sigma_H$). In local Cartesian coordinates $(x, y, z)$ the $z$-axis is positive downward and is parallel to a vertical field line. Regions 1 ($z>0$) and 2 ($z<0$) represent respectively a uniform cold magnetosphere with the Alfvén speed $V_1$ and a non-conducting neutral atmosphere. In such a simplified model (hereafter we call it a simple injection model), a problem of the transmission, reflection, and mode conversion of the vertically incident HM-wave with the sinusoidal structure defined by the perpendicular wave number $k_\perp$ has been formulated separately for two cases of the incidence of the shear Alfvén wave and the magnetosonic wave by TAMAO (private communication, 1983). In the following, let us introduce a notation with double suffices, $B_{Ij}$, to represent the intensity of the perturbed magnetic induction: we use the first capital suffix "I" for the mode classification, *i.e.*, "A" and "F" for the Alfvén and the fast waves in region 1 and "P" for the transmitted magnetic poloidal mode in region 2, respectively. The second suffix "j", which takes either "u" or "d", specifies the direction of vertical propagation, "upgoing" or "downgoing".

2.1.1. The shear Alfvén wave incidence

Intensities of the tangential magnetic field of the reflected Alfvén wave, the converted fast wave, and the transmitted poloidal mode, which are normalized by the incident Alfvén wave intensity, are given by the following expressions,

$$B_{\mathrm{Au}}/B_{\mathrm{Ad}}=-h_{\mathrm{A}}(\bar{k}_{\perp},\bar{\omega})/g(\bar{k}_{\perp},\bar{\omega})\ , \tag{1}$$

$$B_{\mathrm{Fu}}/B_{\mathrm{Ad}}=-2\bar{k}_{\parallel}\bar{\Sigma}_{\mathrm{H}}/g(\bar{k}_{\perp},\bar{\omega})\ , \tag{2}$$

and

$$B_{\mathrm{Pd}}/B_{\mathrm{Ad}}=-2i\bar{k}_{\perp}\bar{\Sigma}_{\mathrm{H}}/g(\bar{k}_{\perp},\bar{\omega})\ , \tag{3}$$

with

$$g(\bar{k}_{\perp},\bar{\omega})=i\bar{\omega}\bar{\Sigma}_{\mathrm{H}}^{2}-(\bar{\Sigma}_{\mathrm{P}}+1)(\bar{k}_{\perp}-i\bar{k}_{\parallel}-i\bar{\omega}\bar{\Sigma}_{\mathrm{P}})\ , \tag{4}$$

and

$$h_{\mathrm{A}}(\bar{k}_{\perp},\bar{\omega})=i\bar{\omega}\bar{\Sigma}_{\mathrm{H}}^{2}-(\bar{\Sigma}_{\mathrm{P}}-1)(\bar{k}_{\perp}-i\bar{k}_{\parallel}-i\bar{\omega}\bar{\Sigma}_{\mathrm{P}})\ . \tag{5}$$

In the above, notations with a lateral bar at the top are non-dimensional quantities, and $k_{\parallel}=[(\omega/V_1)^2-k_{\perp}^2]^{1/2}$ is the parallel wave number of the fast wave with a frequency $\omega$. For normalization we have used a thickness $D$ and an Alfvén speed $V_2$ of a trapping region, which will be introduced later in a 5-layer model, as the standard length and the velocity. Height-integrated conductivities are thus normalized in terms of $\mu_0 V_2$.

Equations (2) and (3) indicate that both converted fast wave and transmitted poloidal mode disappear for $\bar{\Sigma}_{\mathrm{H}}=0$. In other words, the direct origin of ground magnetic signatures is the Hall current induced by the shear Alfvén wave incidence. Numerical examples of variations of three intensity ratios given by eqs. (1)–(3) *versus* a change of $\bar{\Sigma}_{\mathrm{H}}$ or $\bar{\Sigma}_{\mathrm{P}}$ are shown in Fig. 1a ($\bar{\Sigma}_{\mathrm{P}}=1$) and Fig. 1b ($\bar{\Sigma}_{\mathrm{H}}=1$) for $\bar{\omega}=2$ and $\bar{k}_{\perp}=10$. As is seen in Fig. 1a, the transmitted magnetic signal intensity becomes larger than the incident one in some range of $\bar{\Sigma}_{\mathrm{H}}$. Except for the special case of $\bar{\Sigma}_{\mathrm{P}}=1$, the reflection of the Alfvén wave usually occurs even for $\bar{\Sigma}_{\mathrm{H}}=0$. Whereas an increase of $\bar{\Sigma}_{\mathrm{P}}$ results in a decrease of the transmitted signal as shown in Fig. 1b.

2.1.2. The fast wave incidence

Similarly, the relative intensities of the reflected fast wave, converted Alfvén wave, and transmitted poloidal mode have been derived at the time of the fast wave incidence, and are given as

$$B_{\mathrm{Au}}/B_{\mathrm{Fd}}=-2\bar{\omega}\bar{\Sigma}_{\mathrm{H}}/g(\bar{\omega},\bar{k}_{\perp})\ , \tag{6}$$

$$B_{\mathrm{Fu}}/B_{\mathrm{Fd}}=-h_{\mathrm{F}}(\bar{\omega},\bar{k}_{\perp})/g(\bar{\omega}\ ,\bar{k}_{\perp})\ , \tag{7}$$

and

$$B_{\mathrm{Pd}}/B_{\mathrm{Fd}}=2i\bar{k}_{\perp}(\bar{\Sigma}_{\mathrm{P}}+1)/g(\bar{\omega},\bar{k}_{\perp})\ , \tag{8}$$

where

$$h_{\mathrm{F}}(\bar{\omega},\bar{k}_{\perp})=i\bar{\omega}\bar{\Sigma}_{\mathrm{H}}^{2}-(\bar{\Sigma}_{\mathrm{P}}+1)(\bar{k}_{\perp}+i\bar{k}_{\parallel}-i\bar{\omega}\bar{\Sigma}_{\mathrm{P}})\ . \tag{9}$$

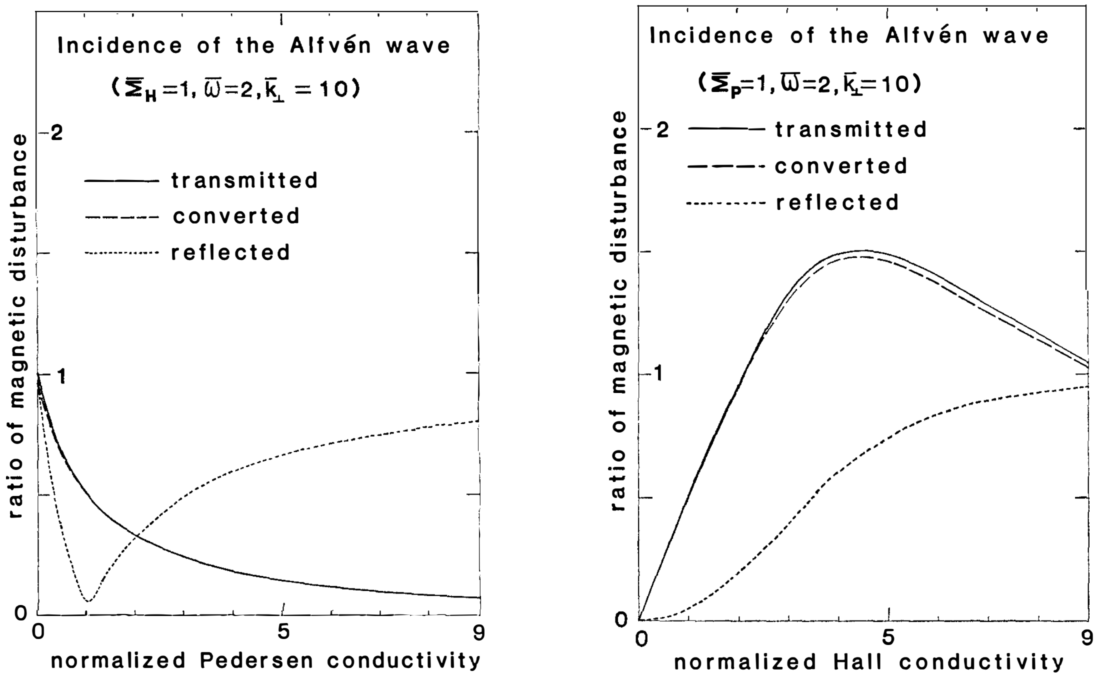


(*a*) (*b*)

*Fig. 1.* *Rates of the reflection, $B_{Au}/B_{Ad}$ (dotted line), conversion, $B_{Fu}/B_{Ad}$ (broken line), and transmission, $B_{Pd}/B_{Ad}$ (full line) of the incident Alfvén wave with the perpendicular wave number $\bar{k}_\perp=10$ and the frequency $\bar{\omega}=2$ versus conductivity variations: (a) The fixed $\bar{\Sigma}_H=1$ and a variable $\bar{\Sigma}_P$, (b) the fixed $\bar{\Sigma}_P=1$ and a variable $\bar{\Sigma}_H$.*

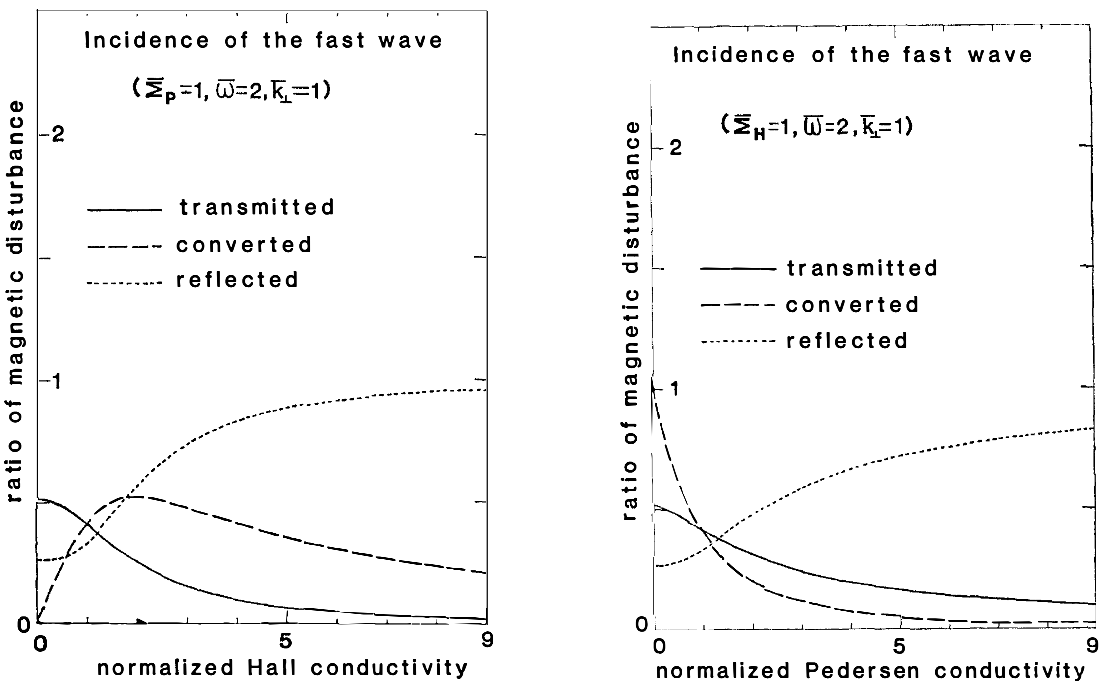


(*a*) (*b*)

*Fig. 2.* *Similar to Fig. 1 but for the vertial incidence of the fast wave. Magnetic signal intensities are normalized by the intensity of the incident fast wave.*

In Figs. 2a and 2b we illustrate the conductivity dependences of three magnetic field intensity ratios given by eqs. (6)–(8) for the incidence of the fast wave with the same parameters as those in Fig. 1. In both figures there are such tendency that the transmission signal intensity decreases with an increase in conductivities whereas the reflection efficiency of the fast wave increases. Thus, the magnetic field of the fast wave is screened more or less by the $E$-layer. This tendency is understandable quite naturally, because the inductive electric field of the fast wave is solenoidal that induces the eddy Pedersen current in the ionosphere.

### 2.2. *A localized injection model with a trapping layer*

Next let us examine the modification of ionospheric response due to the presence of a trapping region of the fast wave, as well as the consequence of localization of the incident shear Alfvén wave. Let us call here a model case for such interaction as the localized injection model (FUJITA and TAMAO, 1984, 1985). The model consists of a semi-infinite magnetosphere (region 1), a trapping upper ionosphere (region 2) with a thickness $D$ and an Alfvén speed $V_2$, a current sheet $E$-layer, a neutral atmosphere with a thickness $h$, and a semi-infinitely extending solid earth. The electrostatic potential of the incident Alfvén wave has a Gaussian form with a horizontal characteristic length $r_0$.

We have made numerical calculation to obtain the horizontal magnetic field intensities of the reflected Alfvén, the trapped fast waves and the transmitted poloidal mode at the levels just above and below the $E$-layer. Some numerical results at $\bar{r}=$

*Table 1. Intensities of the horizontal magnetic field of several modes associated with the incidence of the shear Alfvén wave with $\bar{\omega}=2$ evaluated in two model cases. Those for a localized injection model with a source size $\bar{r}_0=0.1$ and determined at $\bar{r}=0.01$ are given in the upper row for each value of $\bar{\Sigma}_H$ or $\bar{\Sigma}_P$, while field intensities obtained for a simple injection model with $\bar{k}_\perp=1/\bar{r}_0=10$ are given in the lower row.*

(a) $\bar{\Sigma}_H=1$, 2 and 5 with a fixed value of $\bar{\Sigma}_P=1$

| $\bar{\Sigma}_H$ | $B_{Fd}$ | $B_{Fu}$ | $B_{Ad}$ | $B_{Au}$ | $B_{Pd}$ | $B_{Pu}$ |
|---|---|---|---|---|---|---|
| 1 | 1.98E-6 | 4.91E−1 | 1 | 2.16E−2 | 5.00E−1 | 6.66E−3 |
| | — | 4.89E−1 | 1 | 4.99E−2 | 4.99E−1 | — |
| 2 | 3.05E-6 | 9.73E−1 | 1 | 8.60E−2 | 9.90E−1 | 1.33E−2 |
| | — | 9.47E−1 | 1 | 1.93E−1 | 9.68E−1 | — |
| 5 | 2.19E-6 | 2.06E+0 | 1 | 4.45E−1 | 2.09E+0 | 2.42E−2 |
| | — | 1.46E+0 | 1 | 7.47E−1 | 1.49E+0 | — |

(b) $\bar{\Sigma}_P=1$, 2 and 5 with a fixed value of $\bar{\Sigma}_H=1$

| $\bar{\Sigma}_P$ | $B_{Fd}$ | $B_{Fu}$ | $B_{Ad}$ | $B_{Au}$ | $B_{Pd}$ | $B_{Pu}$ |
|---|---|---|---|---|---|---|
| 1 | 1.98E−6 | 4.91E−1 | 1 | 2.16E−2 | 5.00E−1 | 6.66E−3 |
| | — | 4.89E−1 | 1 | 4.99E−2 | 4.99E−1 | — |
| 2 | 9.89E−7 | 3.26E−1 | 1 | 3.35E−1 | 3.32E−1 | 4.33E−3 |
| | — | 3.21E−1 | 1 | 3.39E−1 | 3.28E−1 | — |
| 5 | 2.22E−7 | 1.59E−1 | 1 | 6.67E−1 | 1.62E−1 | 1.97E−3 |
| | — | 1.46E−1 | 1 | 6.69E−1 | 1.49E−1 | — |

0.01 (the horizontal radial distance from the injection center) obtained for normalized parameters, $\bar{h}=0.1$, $\bar{r}_0=0.1$, $\bar{V}_1=4$, and $\bar{\sigma}_G$ (conductivity in the solid earth)$=1000$ are given in Table 1a (for the fixed $\bar{\Sigma}_P=1$) and Table 1b ($\bar{\Sigma}_H=1$). Other parameters employed are the same as those used in the previous section. For comparison we also present the corresponding intensity values calculated for the simple injection model. For each of three different values of $\bar{\Sigma}_H$ (Table 1a) or $\bar{\Sigma}_P$ (Table 1b), the intensities obtained in the localized and the simple injection models are shown in the upper and the lower rows, respectively. We can see there is no significant difference between the two model cases except for values of $B_{Au}/B_{Ad}$ for a case of $\bar{\Sigma}_P=1$. In this special case we have confirmed that there still remain differences in $B_{Au}/B_{Ad}$ between the two models even for the limit of $\sigma_G=0$ and $V_1=V_2$, and thus this discrepancy must be attributed to the localization of the incident wave. Except for this point the trapping effect of the fast waves has no appreciable modification on the ionospheric response in the near-source region.

### 2.3. *A ducted model of the fast wave*

The fast wave, which is secondarily generated by the induced Hall current associated with the localized injection of the Alfvén wave, can propagate horizontally crossing field lines and reach lower latitudes as waveguide modes in the trapping layer. Dispersion characteristics and energetics of the absorption of ducted modes in the 5-layer model have been studied in detail (FUJITA, 1985). We assume here that the eigen-modes oscillations satisfying the dispersion relation of the ducted fast waves and their associated Alfvén and transmitted poloidal modes can reach lower latitudes without the strong absorption. We now call such eigen-mode propagation in a region far away from the injection source the ducted model case.

In such a model, we have numerically determined the perpendicular eigen wave number for the ducted mode which yields the same normalized frequency as that ($\bar{\omega}=2$) of the incident shear Alfvén wave for the localized injection model. We have then calculated intensities of EM-fields of each mode with the above perpendicular wave number at the horizontal position $\bar{r}=4$. The intensities are normalized by the horizontal intensity of the downgoing fast wave obtained at the level just above the $E$-layer at this time, and are shown in Tables 2a ($\bar{\Sigma}_P=1$) and 2b ($\bar{\Sigma}_H=1$) based on similar rules as those in Table 1. Simultaneously shown are the corresponding field intensities estimated by making use of the simple injection model with the vertical incidence of the fast wave with the same perpendicular wave number and frequency as those of the ducted model. We can extract several features of the ionospheric response in the ducted model from a comparative examination of intensities in Table 2. For instance, $B_{Ad}/B_{Au}$ is always very close to $(V_1-V_2)/(V_1+V_2)=0.6$, irrespective of the values of the height-integrated conductivities. However, $B_{Pd}/B_{Fd}$ decreases with an increase in both $\bar{\Sigma}_H$ and $\bar{\Sigma}_P$, and such a tendency is also seen among corresponding values in the simple injection model. Thus, magnetic signals are always screened partially by the $E$-layer for fast wave incidence even in the ducted model. But $B_{Pd}/B_{Fd}$ in the ducted model is much larger than that in the simple injection case as shown in Table 2, because of the presence of the reflecting solid earth in the former.

*Table 2. Intensities of the horizontal magnetic field of several modes associated with the incidence of the fast wave with $\bar{\omega}=2$, obtained in a ducted model at $\bar{r}=4$ (an upper row) and in a simple injection mode with $\bar{k}_{\perp}=10$ (a lower row). For further details see the text.*

(a) $\bar{\Sigma}_H=1$, 2 and 5 with $\bar{\Sigma}_P=1$

| $\bar{\Sigma}_H$ | $B_{Fd}$ | $B_{Fu}$ | $B_{Ad}$ | $B_{Au}$ | $B_{Pd}$ | $B_{Pu}$ |
|---|---|---|---|---|---|---|
| 1 | 1 | 8.54E−1 | 1.23E−1 | 2.05E−1 | 9.72E−1 | 7.90E−1 |
| | 1 | 3.08E−1 | — | 4.17E−1 | 3.77E−1 | — |
| 2 | 1 | 7.79E−1 | 2.42E−1 | 4.03E−1 | 9.53E−1 | 7.78E−1 |
| | 1 | 5.43E−1 | — | 5.17E−1 | 2.31E−1 | — |
| 5 | 1 | 8.38E−1 | 2.94E−1 | 4.90E−1 | 4.55E−1 | 3.85E−1 |
| | 1 | 8.70E−1 | — | 3.47E−1 | 5.10E−2 | — |

(b) $\bar{\Sigma}_P=1$, 2 and 5 with $\bar{\Sigma}_H=1$

| $\bar{\Sigma}_P$ | $B_{Fd}$ | $B_{Fu}$ | $B_{Ad}$ | $B_{Au}$ | $B_{Pd}$ | $B_{Pu}$ |
|---|---|---|---|---|---|---|
| 1 | 1 | 8.54E−1 | 1.23E−1 | 2.05E−1 | 9.72E−1 | 7.90E−1 |
| | 1 | 3.08E−1 | — | 4.17E−1 | 3.77E−1 | — |
| 2 | 1 | 7.97E−1 | 8.18E−2 | 1.36E−1 | 8.51E−1 | 6.97E−1 |
| | 1 | 4.55E−1 | — | 2.07E−1 | 2.73E−1 | — |
| 5 | 1 | 8.16E−1 | 3.19E−2 | 5.32E−2 | 5.97E−1 | 4.96E−1 |
| | 1 | 6.99E−1 | — | 5.50E−2 | 1.35E−1 | — |

### *2.4. Behaviour in the intermediate region*

Performing the similar numerical integration as made in the localized injection model to more extending horizontal distances, FUJITA and TAMAO (1985) have shown that the magnetic intensity of the induced fast wave at the level just above the *E*-layer exceeds that of the Alfvén wave beyond the horizontal distance, $r/r_0=3$. With the same parameters as those used in the localized injection model we have obtained magnetic field intensities of all of associated modes at $\bar{r}=0.4$, and the results are listed in Table 3a ($\bar{\Sigma}_P=1$) and Table 3b ($\bar{\Sigma}_H=1$). Here every intensity is normalized in terms of the intensity of the upgoing fast wave which is the most dominant in the intermediate range of distances from the injection source. In this case, too, $B_{Ad}/B_{Au}$ is nearly equal to 0.6 as in the ducted model, because of no primary incident Alfvén wave in this region. Whereas the behaviour of $B_{Fd}/B_{Fu}$ is different from that in the distant region, so we speculate that there still remain induced fast waves which are not the constituent of the normal ducted modes, and that magnetic intensities are made up from different amount of contributions of different wave numbers, particularly due to the assumed finite horizontal size of the injected wave. Other remarkable behaviours seen from Table 3 are: $B_{Au}/B_{Fu}$ increases with $\bar{\Sigma}_H$ but decreases with increasing of $\bar{\Sigma}_P$. $B_{Pd}/B_{Fu}$ increases with an increase in both $\bar{\Sigma}_H$ and $\bar{\Sigma}_P$, while $B_{Pu}/B_{Fu}$ decreases with both $\bar{\Sigma}_H$ and $\bar{\Sigma}_P$.

Finally, for understanding different ionospheric response in different horizontal ranges from the injection source, conductivity-dependence curves of a total horizontal magnetic field intensity ratio obtained at just below and above the *E*-layer, which gives us a crude measure of the ionospheric shielding, are shown in Fig. 3 for three different

*Table 3. Horizontal magnetic field intensities of several modes determined at $\bar{r}=0.4$ (intermediate region), by using a localized injection model with the same parameters as those of Table 1.*

(a) $\bar{\Sigma}_H=1$, 2 and 5 with $\bar{\Sigma}_P=1$

| $\bar{\Sigma}_H$ | $B_{Fd}$ | $B_{Fu}$ | $B_{Ad}$ | $B_{Au}$ | $B_{Pd}$ | $B_{Pu}$ |
|---|---|---|---|---|---|---|
| 1 | 1.40E−3 | 1 | 1.32E−1 | 2.13E−1 | 2.87E−1 | 8.46E−1 |
| 2 | 1.19E−3 | 1 | 2.48E−1 | 4.10E−1 | 5.00E−1 | 7.77E−1 |
| 5 | 2.16E−4 | 1 | 2.45E−1 | 4.09E−1 | 8.38E−1 | 2.47E−1 |

(b) $\bar{\Sigma}_P=1$, 2 and 3 with $\bar{\Sigma}_H=1$.

| $\bar{\Sigma}_P$ | $B_{Fd}$ | $B_{Fu}$ | $B_{Ad}$ | $B_{Au}$ | $B_{Pd}$ | $B_{Pu}$ |
|---|---|---|---|---|---|---|
| 1 | 1.40E−3 | 1 | 1.32E−1 | 2.13E−1 | 2.87E−1 | 8.46E−1 |
| 2 | 1.11E−3 | 1 | 8.61E−2 | 1.36E−1 | 3.96E−1 | 7.21E−1 |
| 5 | 6.26E−4 | 1 | 3.51E−2 | 5.31E−2 | 5.74E−1 | 4.88E−1 |

horizontal positions: $\bar{r}=0.01$ (the source region), $\bar{r}=0.4$ (the intermediate region), and $\bar{r}=4$ (the distant ducted region). In the left panel variations on $\bar{\Sigma}_H$ with the fixed $\bar{\Sigma}_P=1$ are given, while those on $\bar{\Sigma}_P$ with $\bar{\Sigma}_H=1$ are demonstrated in the right panel. It is a remarkable tendency that the magnetic intensity in a region below the ionosphere becomes larger than that at the level above the *E*-layer in the source region when $\bar{\Sigma}_H$ takes a large value. On the other hand, the screening effect in the source region is rather strong for large values of $\bar{\Sigma}_P/\bar{\Sigma}_H$. In the intermediate and distant regions, be-

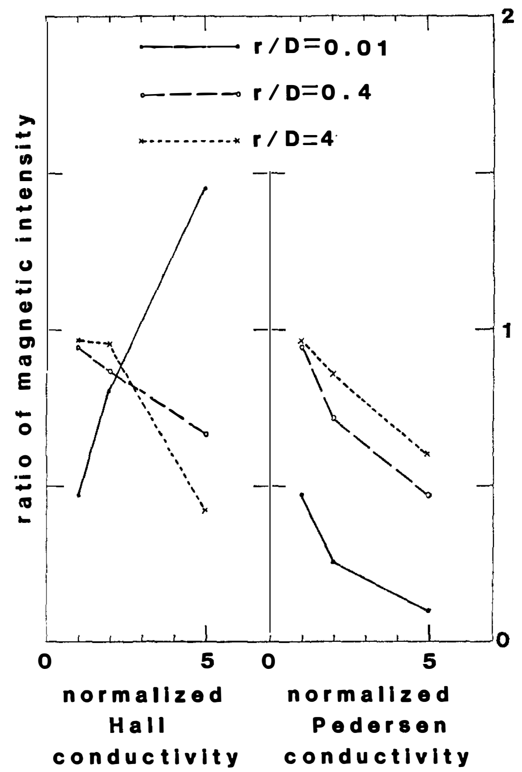


*Fig. 3. Conductivity dependences of a ratio of the total horizontal magnetic field intensities at two altitudes just below and above the E-layer for three positions with different horizontal distances from the injection center, $\bar{r}=0.01$ (a near-source region, full line), $\bar{r}=0.4$ (an intermediate region, broken line), and $\bar{r}=4$ (a distant region, dotted line). In the left panel, $\bar{\Sigma}_H$ is a variable for $\bar{\Sigma}_P=1$ while $\bar{\Sigma}_P$ is a variable with $\bar{\Sigma}_H=1$ in the right panel.*

haviour of the ratios is similar to each other, and the ionospheric shielding is relatively weak for $\bar{\Sigma}_H \simeq \bar{\Sigma}_P \simeq 1$.

## 3. Conclusions

From aspects of origin and transportation of pc 1 geomagnetic pulsation signals, we have comparatively studied characteristics of the ionospheric response to incident HM-waves by postulating three different model cases, *i.e.*, (i) a simple injection model of the vertical incidence of the shear Alfvén and the fast waves with a sinusoidal horizontal structure, (ii) a localized injection model of the shear Alfvén wave, and (iii) a ducted model of the fast waves. The first is the most simplified one, consisting of two semi-infinite magnetospheric and atmospheric layers interfaced by an anisotropic conducting sheet, to describe the reflection, mode conversion, and transmission of the incident signal by the ionosphere. Both second and third models are composed of 5-layers including a trapping upper ionosphere and a reflecting solid earth. The second model with the localized incidence of the shear Alfvén wave has been introduced to deal with the ionospheric response in a near-source region in high latitudes, while the third model is an appropriate one for the horizontal spread of HM-signals in a far away region from the source. In the intermediate range of horizontal distances we have extensively applied the similar calculations as those made in the source region, and have shown that the fast wave generated by the ionospheric Hall current becomes dominant over the shear Alfvén wave in the intermediate region.

We have considered ionospheric effects on HM-waves by examining the behaviour of magnetic signal intesities at two levels just above and below the ionospheric *E*-layer. The main results obtained are summarized as follows:

(1) In the source region the ionospheric response to the reflection and transmission of the shear Alfvén wave are nearly the same for the simple injection and the localized injection models. Hence, we conclude that the effects of localization of the incident wave can be represented by the simple sinusoidal model with the same horizontal scale-length as the localized source.

(2) In the intermediate and distant regions the magnetic signal behaviour due to the ducted wave propagation is essential, and so the simple injection model of the fast wave without a trapping is not sufficient to describe such behaviour.

(3) The ionospheric screening effect is not significant in the intermediate and distant regions, when both $\bar{\Sigma}_H$ and $\bar{\Sigma}_P$ do not much exceed unity. Whereas the shielding in the source region is significant when $\bar{\Sigma}_P$ is larger than $\bar{\Sigma}_H$, but the horizontal magnetic intensity at the level just below the ionosphere exceeds that at the level above the ionosphere if the Hall conductivity is larger than the Pedersen conductivity.

## Acknowledgments

The author would like to express his gratitude to Prof. T. TAMAO, University of Tokyo, for stimulating discussion, criticism, and continuous encouragement through the course of this study. He is also thankful to Dr. A. HARADA, Director of Kakioka Magnetic Observatory, for his encouragement. A part of numerical computation in

this study has been done with a remote batch system of the Meteorological Research Institute, installed at Kakioka Magnetic Observatory.

## References


FUJITA, S. (1985): Ducted propagation of hydromagnetic waves in the upper ionosphere; 2. Dispersion characteristics and loss mechanism. submitted to J. Geophys. Res.

FUJITA, S. and TAMAO, T. (1984): Interaction of a localized shear Alfvén wave with the anisotropic conducting ionosphere; Behaviour in a near-source region. Mem. Natl Inst. Polar Res., Spec. Issue, **31**, 82–95.

FUJITA, S. and TAMAO, T. (1985): Ducted propagation of hydromagnetic waves in the upper ionosphere; 1. Ionospheric response to the incidence of the localized shear Alfvén wave in high latitudes. submitted to J. Geophys. Res.

GREIFINGER, P. (1972): Micropulsations from a finite source. J. Geophys. Res., **77**, 2392–2396.

GREIFINGER, C. and GREIFINGER, P. (1965): Transmission of micropulsations through the lower ionosphere. J. Geophys. Res., **70**, 2217–2231.

GREIFINGER, C. and GREIFINGER, P. S. (1968): Theory of hydromagnetic propagation in the ionospheric waveguide. J. Geophys. Res., **73**, 7473–7490.

NISHIDA, A. (1964): Ionospheric screening effect and storm sudden commencement. J. Geophys. Res., **69**, 1861–1874.

TAMAO, T. (1964): The structure of three-dimensional hydromagnetic waves in a uniform cold plasma. J. Geomagn. Geoelectr., **16**, 89–114.


*(Received June 2, 1984; Revised manuscript received January 23, 1985)*